5-*tert*-Butyl-*N*-pyrazol-4-yl-4,5,6,7-tetrahydrobenzo[*d*]isoxazole-3-carboxamide Derivatives as Novel Potent Inhibitors of *Mycobacterium tuberculosis* Pantothenate Synthetase: Initiating a Quest for New Antitubercular Drugs

Subash Velaparthi,[†] Michael Brunsteiner,[†] Reaz Uddin,[†] Baojie Wan,[‡] Scott G. Franzblau,[‡] and Pavel A. Petukhov*,[†]

Department of Medicinal Chemistry and Pharmacognosy and Institute for Tuberculosis Research, College of Pharmacy, University of Illinois at Chicago, 833 South Wood Street, Chicago, Illinois 60612

Received November 1, 2007

Abstract: Pantothenate synthetase (PS) is one of the potential new antimicrobial targets that may also be useful for the treatment of the nonreplicating persistent forms of *Mycobacterium tuberculosis*. In this Letter we present a series of 5-*tert*-butyl-*N*-pyrazol-4-yl-4,5,6,7-tetrahydrobenzo[*d*]isoxazole-3-carboxamide derivatives as novel potent *Mycobacterium tuberculosis* PS inhibitors, their in silico molecular design, synthesis, and inhibitory activity.

One-third of the world's human population is thought to be infected with *Mycobacterium tuberculosis* (Mtb), and there are 8 million new cases of tuberculosis (TB) each year.[1] Strains of Mtb resistant to existing drugs are found in nearly every country and a percentage of these are resistant to multiple drugs, making effective treatment extremely expensive and in many cases impossible. One of the hallmarks of Mtb is persistence where sub-population of the bacteria is not actively growing and overall metabolic activity is down-regulated, often termed nonreplicating persistence (NRP). Most currently available drugs are not effective against NRP-Mtb, thus requiring a minimum of 6 months of therapy to prevent relapse. Long-term chemotherapy inevitably increases the risk of drug resistance. Therefore, the discovery and development of drugs effective against NRP-Mtb are considered the highest priority among TB drug discovery efforts.

Ample clinical evidence and animal model data have shed light on the mechanism(s) of persistent infection.[2–4] After the Mtb genome was completed in 1998,[5] subsequent functional genomics and proteomics studies further assisted our understanding of this critical growth phase and have collectively identified over 200 potential targets[6–10] involved in alternative biosynthesis pathways during NRP.

Pantothenate synthetase (PS[a]) catalyzes amide bond formation of pantothenate from D-pantoate and β-alanine accompanied by hydrolysis of Mg-ATP into AMP and Mg-PP$_i$.[11] Pantothenate is a key precursor of coenzyme A and acyl carrier protein, essential for many intracellular processes including fatty acid metabolism, cell signaling, and synthesis of polyketides and nonribosomal peptides. A *PanC* gene knockout (KO) of PS in Mtb results in a highly attenuated phenotype in immunocompromised SCID mice and in immunocompetent BALB/c mice,[12] whereas the Δ*lysA* Δ*panCD* KO mutant exhibits substantially reduced replication and persistence.[13] The PS pathway is not present in humans. Taken together, these data suggest that PS is an appropriate target for developing new therapeutics to treat TB. Whether they will also be useful for the treatment of the NRP form of TB would require availability of a diverse set of PS inhibitors to avoid ambiguities associated with KO experiments. Several recent publications[14–16] explored PS as a potential antimicrobial target. Herein, the discovery of novel druglike potent inhibitors of PS is described.

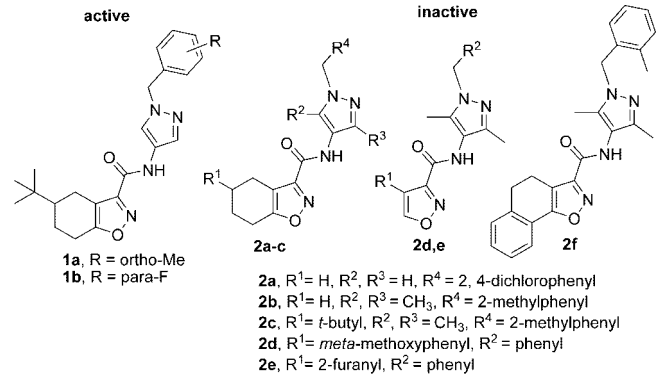

Figure 1. Structures of active compounds **1a** and **1b** and their inactive analogues **2a**−**f**.

Our efforts have started with two screening leads **1a**,**b**. (Figure 1) obtained from an HTS screening of the NIH Molecular Libraries Small Molecule Repository of 10 009 compounds performed by the National Institutes of Health (NIH) Molecular Libraries Screening Centers Network (MLSCN).[17]

A substructure search in the screened database of 10 009 compounds for scaffold **2** resulted in eight analogues **2a**−**f** (Figure 1). A comparison of the active compounds **1a**,**b** and inactive compounds **2a**−**f** indicated that the presence of a *tert*-butyl group and absence of substituents in positions 3 and 5 of the pyrazole ring are essential for PS inhibitory activity of these ligands.

Crystal structures are available for the apo protein (PDB: 2A88)[18] and a number of complexes with the natural substrate and reaction intermediates.[19] To gain additional insights for further modifications of the active compounds **1a**,**b**, their *R* and *S* enantiomers were docked to the binding site of PS using FRED docking program[20] (Figure 2).

It was found that depending on the number of water molecules kept in the binding site during docking FRED found two major poses (Figure 2), which are similar to those found for the reaction intermediates[19] and nafronyl.[21] In pose A (Figure 2A,B) the tetrahydrobenzoisoxazole ring of (*R*)-**1a** occupies the position of the adenine ring of the reaction intermediate, whereas in pose B (Figure 2C) the molecule is rotated 180° and the tetrahydrobenzoisoxazole ring mimics the position of the pantoyl portion of the reaction intermediate cocrystallized with PS in PDB 1N2H.

* To whom correspondence should be addressed. Phone: 312-996-4174. Fax: 312-996-7107. E-mail: pap4@uic.edu.

† Department of Medicinal Chemistry and Pharmacognosy.

‡ Institute for Tuberculosis Research.

[a] Abbreviations: PS, pantothenate synthetase; ADMET, absorption, distribution, metabolism, excretion, toxicity; SCID, severe combined immuno deficiency; FRED, fast rigid exhaustive docking; EDC, 1-ethyl-3-[3-dimethylaminopropyl]carbodiimide; BOC, *tert*-butyloxycarbonyl; DMAP, 4-dimethylaminopyridine; LORA, low oxygen recovery assay, a screen against nonreplicating bacilli; MABA, microplate Alamar blue assay, a screen against exponentially growing cells.

10.1021/jm701372r CCC: $40.75
Published on Web 03/13/2008

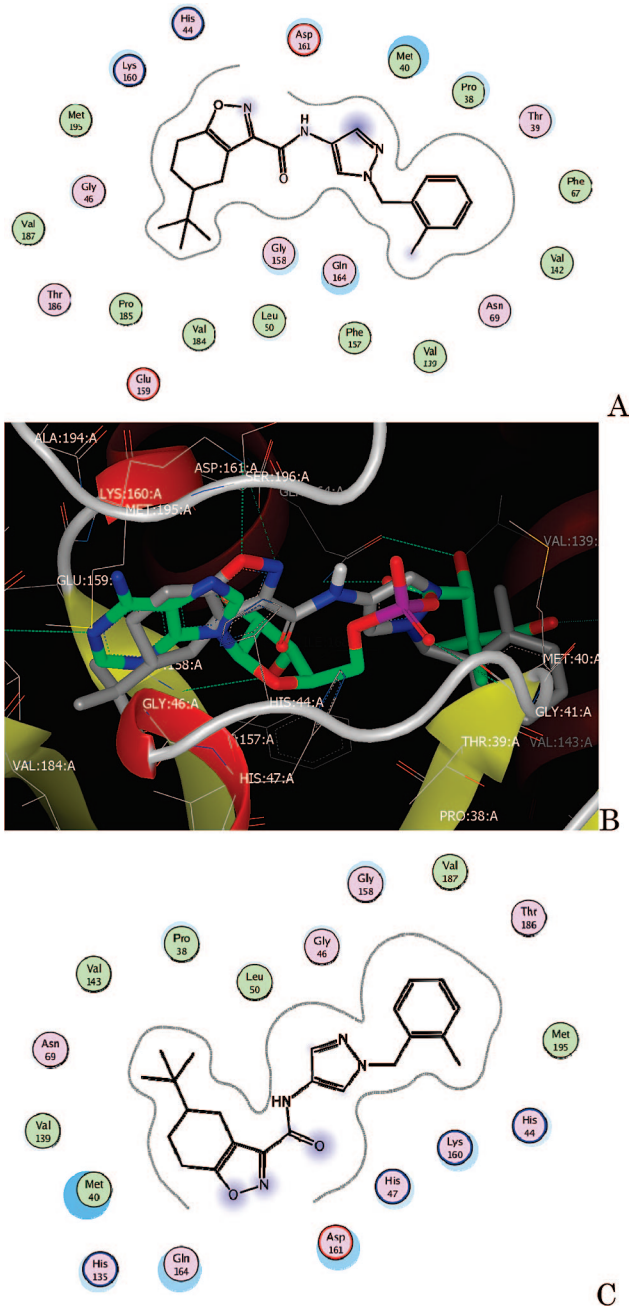

Figure 2. Protein–ligand interaction between (*R*)-**1a** and PS (PDB: 2A88):[22] (green) hydrophobic, (light-purple) polar, (blue ring) basic, (red ring) acidic. The tetrahydrobenzoisoxazole ring of **1a** occupies the position of the adenine ring (A, B) or the position of the pantoyl portion (C) of the reaction intermediate cocrystallized with PS in PDB 1N2H.[19]

In both poses the *tert*-butyl group is buried in the hydrophobic pockets formed by five hydrophobic residues: Met[195], Val[187], Pro[185], Val[184], Leu[50] in pose A and Met[40], Val[139], Val[143], Pro[38], Leu[50] in pose B. The similarity of the FRED scores does not allow us to prioritize at a definitive level one of the binding poses over the other. The binding of the *tert*-butyl group in hydrophobic pockets of the binding site is consistent with its importance for inhibitory activity of the ligands. For **1b** only one binding pose, corresponding to the pose A of **1a**, was found. The binding poses of the *S*-isomers of **1a** and **1b** (not shown) were found to be similar to those of *R*-isomers.

To evaluate whether the area of the binding site occupied by the phenyl ring of **1a**,**b** can accommodate larger and more polar

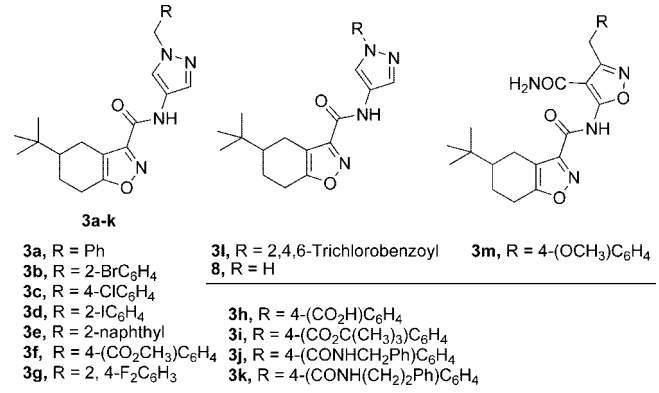

Figure 3. Structures of active compounds **3a**−**m**.

Scheme 1[a]

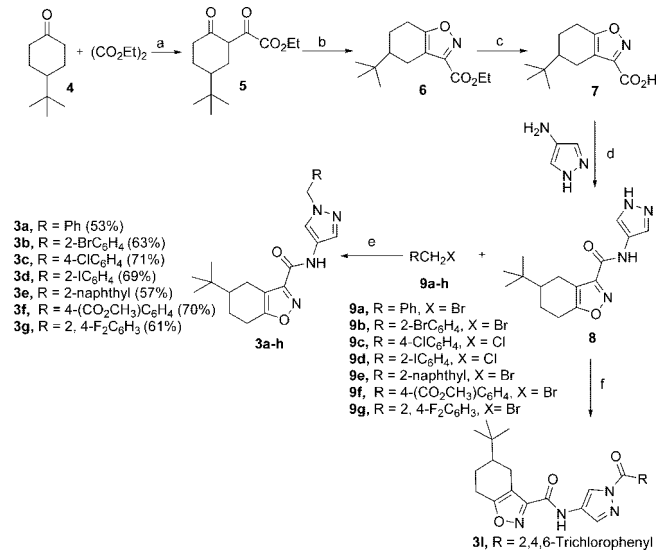

[a] Reagents and conditions: (a) NaOEt, EtOH, 4 h, reflux, 52%; (b) $NH_2OH \cdot HCl$, EtOH, 1 h, reflux, 78%; (c) 2 N NaOH, MeOH, 1 h, 89%, 0 °C to room temp; (d) EDC, HOBT, DIPEA, CH_2Cl_2, 6 h, 62%; (e) NaH, DMF, 0 °C to room temp; (f) 2,4,6-trichlorobenzoyl chloride, NaH, THF, 0 °C, 1 h, 61%.

substituents and to generate a preliminary SAR, new analogues shown in Figure 3 were designed, synthesized, and tested for PS inhibitory activity.

The synthesis of **3a**−**g** is outlined in Scheme 1 and the Supporting Information. The reaction[23] of ketone **4** with diethyl oxalate in the presence of sodium ethoxide gave ester **5**. Cyclization[24] of **5** with hydroxylamine, hydrolysis of the resulting isoxazole **6**, and coupling of acid **7** with 4-aminopyrazole[25] in the presence of EDC and HOBt yielded pyrazole **8**. The resulting pyrazole **8** was further alkylated by various substituted benzylhalides **9a**−**g** to give final products **3a**−**g**. The reaction of **8** with 2,4,6-trichlorobenzoyl chloride yielded **3l**. Alkaline hydrolysis of ester **3f** gave acid **3h** that was converted to ester **3i** with $(BOC)_2O$ in ^{t}BuOH and DMAP. Coupling of acid **3h** with benzylamine and 2-phenethylamine in the presence of EDC and HOBt yielded **3j** and **3k**, respectively. The treatment of 4-methoxy-β-nitrostyrene and Et_3SiH in dry CH_2Cl_2 with $TiCl_4$ gave arylacetohydroximoyl chloride.[26] It was further converted to the nitrile oxide that was subjected to [3 + 2] cycloaddition with cyanoacetaminde.[27] The resulting 5-amino isoxazole (not shown) was coupled with acid **7** in the presence of EDC and HOBt, leading to **3m**.

Compounds **1a**,**b**, **3a**−**m**, **7**, and **8** were tested for inhibition of PS (Table 1). The assays[16,18] were conducted by the

Table 1. Inhibition of Pantothenate Synthetase (% Inhibition at 100 μM and IC_{50}) and Inhibition of Mtb Growth in MABA and LORA Assays by **1a**,**b**, **2a**, **3a**−**m**, **7**, and **8**

compd	% inhibition at 100 μM	IC_{50} (nM)	% inhibition at 128 μM	
			MABA	LORA
1a	89	$120 \pm 6^{a,c}$	46	15
1b	98	$150 \pm 9^{a,c}$	0	0
2a	18	ND[a,b,d]	70	53
3a	100	97 ± 4^{c}	84	62
3b	94	140 ± 9^{c}	73	24
3c	98	140 ± 9^{c}	ND[b]	ND[b]
3d	84	160 ± 8^{c}	70	12
3e	97	90 ± 1^{c}	43	ND[b]
3f	100	160 ± 1^{c}	48	0
3g	100	130 ± 10^{c}	56	47
3h	99	460 ± 42^{c}	41	2
3i	79	250 ± 8^{c}	ND[b]	ND[b]
3j	82	210 ± 10^{c}	54	46
3k	78	140 ± 8^{c}	19	11
3l	17	ND[b,d]	34	26
3m	79	7130 ± 297^{c}	14	14
7	12	ND[b,d]	5	11
8	43	61000 ± 5700^{c}	60	4

[a] **1a**, **2b**, and **2a** were also tested within the MLSCN/NIH screening program. [b] ND: not done. [c] No inhibition of the control enzyme was observed. [d] Not tested for inhibition of the control enzyme.

Tuberculosis Antimicrobial Acquisition and Coordinating Facility (TAACF) through a research and development contract with the U.S. National Institute of Allergy and Infectious Diseases (NIAID) of the NIH using Rv3602c, EC 6.3.2.1 (*PanC*).

The new analogues in series **3** exhibited activity ranging from IC_{50} of 90 nM to 7.13 μM with the majority of ligands exhibiting activity better than 250 nM. The increase in potency of the ligands in series **3** compared to that of intermediates **7** and **8** suggests that the scaffolds of **7** and **8** alone are too small to exhibit noticeable inhibition and additional substituents in the pyrazole ring are required to improve activity. The best activities, $IC_{50} \leq 100$ nM, are achieved for unsubstituted **3a** and naphthalene-substituted ligand **3e**. Comparison of **3a** with the other compounds in this series suggests that (i) hydrophobic substituents on the benzene ring lead to a slightly increased potency, e.g., **3e** (R = naphthyl) and **1b** (R = 4-FC_6H_4) vs **3i** (R = 4-($CO_2{}^t$Bu)C_6H_4) and **3 h** (R = 4-(CO_2H)C_6H_4), (ii) differences in potency resulting from variation of the substitution pattern on the phenyl ring are not larger than 5-fold. It is unclear why a small R substituent in **1b** (R = 4-FC_6H_4) and a large one in **3k** (R = 4-(CONH(CH_2)$_2$Ph)C_6H_4) result in practically identical potencies even if their docking poses are very different, reflecting the fact that **3k** (as **3j**) is too large to fit into the binding site without parts of the compound protruding from the protein. The fact that **3k** and **3j** exhibit excellent potency suggests that induced fit effects may play an important role in accommodating these compounds in the PS binding site.

Unlike modifications in the phenyl that were relatively insensitive to the size and polarity of the substituents, additional polar moiety in the linker connecting the pyrazole ring with the phenyl ring of **3l** or in the pyrazole ring of **3m** led to a 680-fold decrease in activity of **3m** compared to the activity of **3e** and marginal inhibition of PS by **3l**. The docking of both ligands shows that the newly introduced moieties in **3l** and **3m** are located in the gorge region of the binding site responsible for accommodation of the phosphate group and sugar ring of the reaction intermediate. This may indicate that this area is very sensitive to the nonmatching interactions possibly introduced in **3l** and **3m** or that the extra moieties have changed the spatial arrangement of the key pharmacophore elements of the ligands. It seems that polar and nonpolar moieties in the pyrazole ring result in a decrease in activity as ligand **2c**, which is identical to ligand **1a** with the exception of the two extra methyl groups in the pyrazole ring, showed no inhibition of PS in the MLSCN/NIH screening program.

The MICs of **3a**−**m**, **7**, and **8** in LORA[28] and MABA[29] MIC were found to be larger than 128 μM. The percent of inhibition at 128 μM in LORA and MABA assays is given in Table 1. The inhibition ranges from 0% to 84% in the MABA assay and 62% in the LORA assay and at this high concentration can be affected by the off-target toxicity of the compounds and their metabolites. Several possible reasons for the lack of antimicrobial activity can be suggested, e.g., poor bacterial wall permeability, metabolic stability, or efflux of the inhibitors.

These studies identified *tert*-butyl and pyrazole portions of the PS inhibitors as the two areas containing the key pharmacophore elements. On the other hand, the substituents in the aryl moiety of the pyrazole portion are well tolerated, suggesting that this part of the scaffold is an auxophore, and thus, it may be used to fine-tune ADMET profiles of these compounds. More drastic modifications of the scaffold would be required to determine the binding pose of the inhibitors and address weak MIC, and such efforts are currently under way. These findings are an important step in the development of PS inhibitors and validation of PS as a therapeutic antimicrobial target and potential target for NRP-TB.

Acknowledgment. This research was supported by the NIAID/NIH Grant R21 AI070997 and the Institute for Tuberculosis Research at the University of Illinois at Chicago. PS inhibition assays were funded by the Division of Acquired Immunodeficiency Syndrome of the NIAID/NIH. The financial support for R.U. was provided by the Higher Education Commission of Pakistan. The authors thank OpenEye Scientific Software for providing academic license for the modeling software. We also thank Dr. Alan P. Kozikowski for critical suggestions.

Supporting Information Available: Representative experimental procedures, complete synthetic schemes, and ^{1}H NMR, HRMS, and HPLC data for all target compounds. This material is available free of charge via the Internet at http://pubs.acs.org.

References

(1) Corbett, E. L.; Watt, C. J.; Walker, N.; Maher, D.; Williams, B. G.; Raviglione, M. C.; Dye, C. The growing burden of tuberculosis: global trends and interactions with the HIV epidemic. *Arch. Intern. Med.* **2003**, *163*, 1009–21.

(2) Honer zu Bentrup, K.; Russell, D. G. Mycobacterial persistence: adaptation to a changing environment. *Trends Microbiol.* **2001**, *9*, 597–605.

(3) Wayne, L. G.; Sohaskey, C. D. Nonreplicating persistence of mycobacterium tuberculosis. *Annu. Rev. Microbiol.* **2001**, *55*, 139–163.

(4) Zahrt, T. C. Molecular mechanisms regulating persistent *Mycobacterium tuberculosi*s infection. *Microbes Infect.* **2003**, *5*, 159–167.

(5) Cole, S. T.; Brosch, R.; Parkhill, J.; Garnier, T.; Churcher, C.; Harris, D.; Gordon, S. V.; Eiglmeier, K.; Gas, S.; Barry, C. E., 3rd; Tekaia, F.; Badcock, K.; Basham, D.; Brown, D.; Chillingworth, T.; Connor, R.; Davies, R.; Devlin, K.; Feltwell, T.; Gentles, S.; Hamlin, N.; Holroyd, S.; Hornsby, T.; Jagels, K.; Barrell, B. G.; et al. Deciphering the biology of *Mycobacterium tuberculosis* from the complete genome sequence. *Nature* **1998**, *393*, 537–544.

(6) Sassetti, C. M.; Rubin, E. J. Genetic requirements for mycobacterial survival during infection. *Proc. Natl. Acad. Sci. U.S.A.* **2003**, *100*, 12989–12994.

(7) Bacon, J.; James, B. W.; Wernisch, L.; Williams, A.; Morley, K. A.; Hatch, G. J.; Mangan, J. A.; Hinds, J.; Stoker, N. G.; Butcher, P. D.; Marsh, P. D. The influence of reduced oxygen availability on pathogenicity and gene expression in *Mycobacterium tuberculosis*. *Tuberculosis (Edinb)* **2004**, *84*, 205–217.

(8) Muttucumaru, D. G.; Roberts, G.; Hinds, J.; Stabler, R. A.; Parish, T. Gene expression profile of Mycobacterium tuberculosis in a non-replicating state. *Tuberculosis* **2004**, *84*, 239–246.

(9) Voskuil, M. I.; Visconti, K. C.; Schoolnik, G. K. *Mycobacterium tuberculosis* gene expression during adaptation to stationary phase and low-oxygen dormancy. *Tuberculosis* **2004**, *84*, 218–227.

(10) Cho, S.-H.; Goodleett, D.; Sherman, D.; Franzblau, S. G. ICAT-based comparative proeomic analysis of non-replicating persistent *Mycobacterium tuberculosis*. Manuscript in preparation.

(11) Zheng, R.; Blanchard, J. S. Steady-state and pre-steady-state kinetic analysis of *Mycobacterium tuberculosis* pantothenate synthetase. *Biochemistry* **2001**, *40*, 12904–12912.

(12) Sambandamurthy, V. K.; Wang, X.; Chen, B.; Russell, R. G.; Derrick, S.; Collins, F. M.; Morris, S. L.; Jacobs, W. R., Jr. A pantothenate auxotroph of *Mycobacterium tuberculosis* is highly attenuated and protects mice against tuberculosis. *Nat. Med. (N. Y.)* **2002**, *8*, 1171–1174.

(13) Sambandamurthy, V. K.; Derrick, S. C.; Jalapathy, K. V.; Chen, B.; Russell, R. G.; Morris, S. L.; Jacobs, W. R., Jr. Long-term protection against tuberculosis following vaccination with a severely attenuated double lysine and pantothenate auxotroph of *Mycobacterium tuberculosis*. *Infect. Immun.* **2005**, *73*, 1196–1203.

(14) Tuck, K. L.; Saldanha, S. A.; Birch, L. M.; Smith, A. G.; Abell, C. The design and synthesis of inhibitors of pantothenate synthetase. *Org. Biomol. Chem.* **2006**, *4*, 3598–3610.

(15) Southworth, K.; Sneed, B.; Ross, L.; Cooley, S.; Sosa, M. I.; Manouvakhova, A.; Rasmussen, L.; White, E. L.; Anathan, A.; Fletcher, T. M., III; Goldman, R. C.; Goulding, C.; Eisenberg, D. Identifying Pantothenate Synthetase Inhibitors of *Mycobacterium tuberculosis* from a High Throughput Screen. Presented at the 13th Annual Conference of the Society for Biomolecular Sciences (SBS), Montreal, Canada, 2007.

(16) White, E. L.; Southworth, K.; Ross, L.; Cooley, S.; Gill, R. B.; Sosa, M. I.; Manouvakhova, A.; Rasmussen, L.; Goulding, C.; Eisenberg, D.; Fletcher, T. M., 3rd. 3rd. A novel inhibitor of Mycobacterium tuberculosis pantothenate synthetase. *Journal of Biomolecular Screening* **2007**, *12*, 100–5.

(17) Mycobacterium tuberculosis Pantothenate Synthetase Assay, NIH BioAssay. http://pubchem.ncbi.nlm.nih.gov/assay/assay.cgi?aid=375.

(18) Wang, S.; Eisenberg, D. Crystal structure of the pantothenate synthetase from Mycobacterium tuberculosis, snapshots of the enzyme in action. *Biochemistry* **2006**, *45*, 1554–61.

(19) Wang, S.; Eisenberg, D. Crystal structures of a pantothenate synthetase from M. tuberculosis and its complexes with substrates and a reaction intermediate. *Protein Sci.* **2003**, *12*, 1097–108.

(20) *FRED 2.2, OEChem*, version 1.4.2; OpenEye Scientific Software, Inc.: Santa Fe, NM, 2006; www.eyesopen.com.

(21) White, E. L.; Southworth, K.; Ross, L.; Cooley, S.; Gill, R. B.; Sosa, M. I.; Manouvakhova, A.; Rasmussen, L.; Goulding, C.; Eisenberg, D.; Fletcher, T. M., 3rd. A novel inhibitor of *Mycobacterium tuberculosis* pantothenate synthetase. *J. Biomol. Screening* **2007**, *12*, 100–105.

(22) Parts A and C of Figure 2 were prepared with MOE software (Chemical Computing Group). Part B of Figure 2 was prepared in Vida3 software (OpenEye Inc).

(23) Ingersoll, A. W.; Babcock, S. H. *Organic Synthesis*; Wiley: New York, 1943; Collective Vol. 2, p 531.

(24) Sechi, M.; Sannia, L.; Carta, F.; Palomba, M.; Dallocchio, R.; Dessi, A.; Derudas, M.; Zawahir, Z.; Neamati, N. Design of novel bioisosteres of beta-diketo acid inhibitors of HIV-1 integrase. *Antiviral Chem. Chemother.* **2005**, *16*, 41–46.

(25) Gross, R. S.; Guo, Z.; Dyck, B.; Coon, T.; Huang, C. Q.; Lowe, R. F.; Marinkovic, D.; Moorjani, M.; Nelson, J.; Zamani-Kord, S. Design and synthesis of tricyclic corticotropin-releasing factor-1 antagonists. *J. Med. Chem.* **2005**, *48*, 5780–5793.

(26) Kumaran, G.; Kulkarni, G. H. Synthesis of α-functionalized and nonfunctionalized hydroximoyl chlorides from conjugated nitroalkenes and nitroalkanes. *J. Org. Chem.* **1997**, *62*, 1526–1520.

(27) Beccalli, E. M.; Manfredi, A.; Marchesini, A. Alkynes from 5-aminoisoxazoles. *J. Org. Chem.* **1985**, *50*, 2372–2375.

(28) Cho, S. H.; Warit, S.; Wan, B.; Hwang, C. H.; Pauli, G. F.; Franzblau, S. G. Low-oxygen-recovery assay for high-throughput screening of compounds against nonreplicating *Mycobacterium tuberculosis*. *Antimicrob. Agents Chemother.* **2007**, *51*, 1380–1385.

(29) Collins, L.; Franzblau, S. G. Microplate alamar blue assay versus BACTEC 460 system for high-throughput screening of compounds against *Mycobacterium tuberculosis* and *Mycobacterium avium*. *Antimicrob. Agents Chemother.* **1997**, *41*, 1004–1009.

JM701372R